Journal of Molecular Catalysis A: Chemical 304 (2009) 40–46

Contents lists available at ScienceDirect

Journal of Molecular Catalysis A: Chemical

journal homepage: www.elsevier.com/locate/molcata

Quantitative structure–activity relationship studies on ironporphyrin-catalyzed cyclohexane oxidation with PhIO

Nian Liu, Guo-Fang Jiang, Can-Cheng Guo*, Ze Tan

College of Chemistry and Chemical Engineering, Hunan University, Changsha 410082, PR China

ARTICLE INFO

Article history:
Received 12 October 2008
Received in revised form 14 January 2009
Accepted 14 January 2009
Available online 21 January 2009

Keywords:
Ironporphyrin
Cyclohexane
QSAR
Quantum chemistry
Molecular orbital

ABSTRACT

Quantitative structure–activity relationship (QSAR) studies were performed on the ironporphyrin-catalyzed biomimetic oxidation of cyclohexane. Through quantum chemical calculations, the molecular structures of nine different ironporphyrin catalysts have been optimized and their respective quantum chemical descriptors (FMO energies E_{HOMO}, E_{LUMO}, FMO energy gap DEHL, partition coefficient $\log P$) have been obtained. The ironporphyrin-catalyzed cyclohexane hydroxylation with PhIO was chosen as the model reaction. The yield of cyclohexanol (yield (%)) and the reaction rate constant ($\lg k$) were obtained experimentally, and the reaction kinetics was studied accordingly. 2D-QSAR studies for ironporphyrin catalysts were performed by using multiple linear regression (MLR) analysis. From the established QSAR model equations of $\lg k$, yield (%) and the quantum chemical descriptors ($\lg k = -1.433 + 0.009 \log P - 0.406 E_{LUMO\text{-}b}$ $R = 0.968$ and yield (%) $= 9.556 + 0.500 \log P - 8.997 E_{LUMO\text{-}b}$ $R = 0.821$), we conclude that it is the frontier molecular orbital (FMO) energy level $E_{LUMO\text{-}b}$ which has the most significant effect on the catalytic activity of the ironporphyrins. Further molecular graphics studies and Mulliken's electron population analysis indicated that the energy level of $E_{LUMO\text{-}b}$ can be altered by introducing peripheral substituting groups on the *meso*-phenyl ring. Since the electron withdrawing substituents could lower $E_{LUMO\text{-}b}$ and disperse the electron density of around the centro-metal core of porphyrin better, they can facilitate ironporphyrin's binding with the oxidant and, consequently increase the catalytic activity of ironporphyrin. We also notice that the partition coefficient $\log P$ of ironporphyrin molecule affects the reaction rate and the yield of the cyclohexane hydroxylation reaction as well. Our study may be beneficial for future catalyst design for the metalloporphyrin-catalyzed hydrocarbon oxidations.

1. Introduction

In the past several decades, the behavior of metalloporphyrin-catalyzed hydrocarbon oxidation under mild conditions has been systematically studied as a model of cytochrome P-450 monooxygenase by many researchers [1–11] with the ultimate goal of searching for the most effective metalloporphyrin catalysts for hydrocarbons oxidation [12–14,8,9]. Previous studies showed that the catalytic characteristics of metalloporphyrin catalysts were mainly dependent on the nature of the porphin macrocycle, axial ligand, and the central metal ion [15–18]. For example, the spin and the electron charge of the central metal could be changed with different axial ligands, which could influence the reaction between porphyrin catalyst and the oxidant [19–22]. The variation of substituents on the porphyrin rings may pose steric effects for the oxidant activation on the surface of porphyrin molecule [23–25]. Though major advances have been made on the mechanism of metalloporphyrin-catalyzed biomimetic hydrocarbon oxidation, the optimization of metalloporphyrin catalyst has been largely based on trial and error. The relationship between the catalytic activity of the metalloporphyrin catalyst and their structures and structure-related properties are not well understood. As a result the design of new and better metalloporphyrin catalysts for the oxidation of hydrocarbons through tradition approach has not been very fruitful. Quantitative structure–activity relationship (QSAR) studies have been successfully applied to investigate drugs, enzymes, and biological compounds [26–29] to pinpoint the exact structure-related property which is directly responsible for their specific biological activities, and its application have been very helpful for drug screening and enzyme evolution. But this useful method has been seldom applied on metalloporphyrin-catalyzed reactions and QSAR studies based on quantum chemical calculations are even rarer. To the best of our knowledge, only two cases were reported before. In 2003, QSAR studies based on quantum chemical calculations was used by Lü et al. [30] to investigate the link between the catalyst quantum chemical descriptors and reaction turn over

* Corresponding author. Tel.: +86 731 8821314; fax: +86 731 8821488.
E-mail address: ccguo@hnu.cn (C.-C. Guo).

1381-1169/$ – see front matter © 2009 Elsevier B.V. All rights reserved.
doi:10.1016/j.molcata.2009.01.021

numbers for isobutene oxidation catalyzed by halogenated irontetraphenylporphyrins. A similar study was carried out by Zhang et al. for nitrobenzene oxidation catalyzed by cobalt-porphyrins [31]. These research results have proved that the catalytic activities of metalloporphyrin catalysts correlate well with their individual quantum chemical descriptors, which themselves could be changed due to subtle structural variations. They also proved that QSAR studies on metalloporphyrin-catalyzed reaction based on quantum chemical calculations can be very useful and they supplied valuable theoretical references for the design of more efficient porphyrin catalysts. In this paper, we report the application of 2D QSAR studies on cyclohexane hydroxylation reaction catalyzed by irontetraphenylporphyrin based on quantum chemical calculations.

During the last decades, a series of investigations on the cyclohexane oxidation catalyzed by mono- or bis-metalloporphyrins have been reported by our group [32–34], and the technology based on our group's metalloporphyrin-catalyzed oxidation of cyclohexane has been already applied in industrial KA oil production [35]. Among these investigations, we found that the yield and the rate constant of the cyclohexane hydroxylation reaction have nice Hammett relations with the substituent constant on the porphin rings [33]. Experimental data also implied that the catalytic activities of porphyrins may be affected by more than one structure element of porphyrin. In order to clarify the relevant law of the structure and catalytic activity of metalloporphyrin for better catalyst for the biomimetic oxidation of cyclohexane, quantum chemical calculations and cyclohexane hydroxylation kinetics studies were combined for the first time to perform 2D QSAR studies on the cyclohexane hydroxylation reaction catalyzed by irontetraphenylporphyrin. This QSAR study is based on Hansch–Fujita model, and the main purpose of the present investigation is to assess the impact of frontier molecular orbital (FMO) energies and partition coefficient on the catalytic activities of ironporphyrin-catalyzed cyclohexane hydroxylation reaction.

2. Experimental

2.1. Calculation model and method

Full geometry optimizations for nine irontetraphenylporphyrins with substituent R on the phenyl ring (TRPPFe^{III}Cl) shown in Fig. 1 were performed at semi-empirical PM3 level implemented in the software package Hyperchem 7.0 (Hypercube Inc., USA). There are three kinds of spin states for penta-coordinate ironporphyrin, such as the low-spin $S = 1/2$ state, the intermediate-spin $S = 3/2$ state, and the high-spin $S = 5/2$ state. The spin state and stereochemistry of the iron is controlled by the axial ligands of the penta-coordinate ironporphyrins [19]. The coordination of strong or moderate field ligands leads to low-spin state, while the coordination of weak field ligands leads to high-spin state [19]. Since the axial ligands of all nine ironporphyrins being studied are chlorides, which are moderate field ligands, all nine ironporphyrins are in high-spin state [19,30]. The geometries with high-spin multiplicities ($S = 5/2$) for each ironporphyrin molecule were optimized, respectively, by unrestricted PM3 method (open shell) and equilibrium geometries were identified by vibration analysis. Hyperchem 7.0 software package was also used to compute the QSAR descriptors. Six relevant descriptors (FMO energies $E_{HOMO\text{-}a}$, $E_{HOMO\text{-}b}$, $E_{LUMO\text{-}a}$, $E_{LUMO\text{-}b}$, FMO energy gap DEHL, partition coefficient log P) were generated. All calculations were performed on a Dell 9150 PC (3.8 GHz, 2 GB).

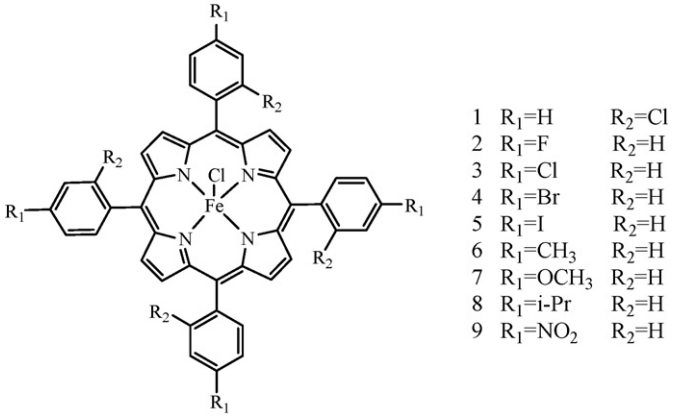

Fig. 1. Molecular structures of irontetraphenylporphyrins TRPPFe^{III}Cl.

2.2. Cyclohexane hydroxylation reaction

2.2.1. Instruments and reagents

^{1}H NMR spectra were recorded on Varian INOVA-400 at 25 °C at 400 MHz with TMS as internal standard. UV–vis spectra were obtained with a PerkinElmer L-17 UV–Vis spectrophotometer. IR spectra were recorded on a PerkinElmer Model 783 IR spectrophotometer. GC analysis was performed on a Shimadzu GC-16A gas chromatography flame ionization instrument. A PerkinElmer 2400 elementary analyzer and a Model 5012 constant temperature water bath were used.

Anhydrous benzene and dichloromethane were used and neutral Al_2O_3 was baked for 5 h at 100 °C. Pyrrole and benzaldehyde were freshly redistilled. PhIO was synthesized via the documented procedures [36], and its purity was measured as 99% by iodimetry. All other reagents were purchased from commercial sources and used without treatment, unless otherwise indicated.

2.2.2. Synthesis of TRPPFe^{III}Cl (1–9)

TRPPFe^{III}Cl (1–9) was synthesized according to the documented procedures [37–39] from the metallization of the *meso*-substituted tetraphenylporphine $TRPPH_2$, the latter was prepared from the condensation of pyrrole and corresponding substituted phenylaldehyde. Their structures were confirmed by ^{1}H NMR, IR spectra, UV–vis spectra and elementary analysis. Spectroscopic data of TRPPFe^{III}Cl 1–9 were consistent with reported data [40–44].

2.2.3. TRPPFe^{III}Cl catalyzed hydroxylation of cyclohexane

Cyclohexane hydroxylation reported in this paper was carried out under nitrogen using the following procedure unless otherwise specified. A mixture of PhIO (100 mg, 4.5×10^{-4} mol), TRPPFeCl (3.0×10^{-5} mol), and cyclohexane (5 ml) in benzene (5 ml) was warmed to 303 K by circulated warm water and stirred for 2 h with an electromagnetic stirrer. The products were analyzed by gas chromatography [45]. Yields were calculated based on PhIO. Samples for kinetics analysis were regularly collected from the reaction system every 10 min with a micro-injector. The reaction mixture was quantified by GC analysis using chlorobenzene as the internal standard and the products were identified by GC–MS.

3. Results and discussion

3.1. Calculation for the structural descriptors of TRPPFe^{III}Cl via quantum chemistry method

The structural descriptors (FMO energies $E_{HOMO\text{-}a}$, $E_{HOMO\text{-}b}$, $E_{LUMO\text{-}a}$, $E_{LUMO\text{-}b}$, FMO energy gap DEHL, partition coefficient log P) of TRPPFe^{III}Cl calculated by unrestricted PM3 method were listed in Table 1. The molecular orbitals were represented in spin-up (a) and spin-down (b) forms because of the open shell method adopted in the calculation and FMO energy levels were represented as $E_{HOMO\text{-}a}$, $E_{HOMO\text{-}b}$, $E_{LUMO\text{-}a}$, and $E_{LUMO\text{-}b}$, accordingly.

Table 1
The data of structural descriptors of TRPPFe^{III}Cl.

TRPPFe^{III}Cl catalyst	log P	E_{HOMO-a} (eV)	E_{HOMO-b} (eV)	E_{LUMO-a} (eV)	E_{LUMO-b} (eV)	DELH (eV)
1	1.046	−6.833	−8.577	−1.772	−3.535	3.298
2	−0.468	−8.323	−8.420	−1.865	−2.009	6.314
3	1.046	−8.217	−8.316	−1.681	−1.905	6.312
4	2.141	−8.028	−8.414	−2.140	−2.354	5.674
5	4.004	−8.234	−8.288	−1.752	−1.925	6.309
6	2.550	−7.944	−7.986	−1.850	−1.696	6.094
7	−2.036	−7.776	−7.877	−1.785	−1.743	5.991
8	5.458	−7.971	−7.980	−1.677	−1.655	6.294
9	−1.323	−8.811	−8.924	−2.507	−2.662	6.149

From the data listed in Table 1, we can see that the ironporphyrins with electron withdrawing groups on the *meso*-phenyl ring have lower E_{LUMO-b} than those with electron donating groups. For example, the E_{LUMO-b} values of T(p-NO_2)PPFe(III)Cl and T(o-Cl)PPFe(III)Cl were smaller than the values of T(p-OCH_3)PPFe(III)Cl and T(p-CH_3)PPFe(III)Cl.

3.2. Kinetic analysis of TRPPFe^{III}Cl catalyzed cyclohexane hydroxylation

For the cyclohexane hydroxylation catalyzed by TRPPFe^{III}Cl [46], the main product of the reaction was cyclohexanol accompanied with trace amount of cyclohexanone. At the temperature tested, a linear relationship could be established between the quantity of cyclohexanol and the reaction time: [cyclohexanol] = $kt + b$ (slope k represented the rate constant of the cyclohexane hydroxylation reaction [47] and higher k value means higher catalytic activity of ironporphyrin catalyst). The equation indicated the oxidation is a zero-order reaction in the initial stages. The cyclohexane oxidation was conducted with nine different catalysts and the cyclohexanol yields and the logarithm values of the reaction rate constants lg k are listed in Table 2. From the data, we can tell that the catalytic performance of ironporphyrin was greatly affected by the substituents because the value of k varied significantly.

3.3. Descriptors investigations and 2D QSAR studies

With the data of six QSAR descriptors of nine irontetraphenylporphyrin derivatives in Table 1 and their respective reaction kinetics for the cyclohexane hydroxylation reaction in Table 2, QSAR studies were performed to establish the relationship between the experimentally observed data and the quantum chemical descriptors related to the physical and chemical properties of the compounds [48]. Attempts were made to correlate the descriptors with the catalytic activity based on the Hansch–Fujita model by multiple linear regressions (MLR) [49]. In the end, we came up with the mathematics expression of lg $1/C = a \log P + bEs + \rho\sigma + d$, where the activity lg $1/C$ is the function of hydrophobic descriptor (log P), the electronic descriptor (Es) and the steric descriptor (σ). And a, b, ρ and d are coefficients in this model.

Table 2
Rate constant lg k and cyclohexanol yield (%) of cyclohexane hydroxylation with TRPPFe^{III}Cl catalysts.

TRPPFe^{III}Cl	lg k [46]	Yield (%) [46]
1	−0.0046	42.85
2	−0.6478	20.05
3	−0.5408	30.50
4	−0.5604	29.14
5	−0.5780	26.53
6	−0.7364	24.35
7	−0.8146	27.85
8	−0.7496	31.20
9	−0.3302	35.04

As we have mentioned previously, the characteristics of ironporphyrin catalysts were influenced by a number of factors. The selection of suitable descriptor correlating to the catalytic activity is the most important step in QSAR modeling. Moreover, in order to avoid the inter-correlated parameters and minimize the information overlap in the QSAR model, a Pearson correlation matrix was used to exclude the interdependence among the descriptors and the catalytic activity indicators in Table 3 [50].

The descriptors with strong inter-correlation ($R > 0.5$) were omitted. Only those descriptors with slight collinear relationship were retained in the same regression equation. The parameters such as correlation coefficient (R), squared correlation coefficient (R^2), variance ratio (F), and standard error of estimate (SEE) were used to assess the statistical qualities of the regression equations. The regression equations with higher R, F value and lower SEE (a statistic of assessing the overall significance) were selected [51]. In the end, two suitable 2D QSAR model equations, each containing two descriptors, were generated with logical mathematics after MLR analysis. Eq. (1) is the correlation of the rate constant lg k with partition coefficient log P and FMO energy E_{LUMO-b} and Eq. (2) is the correlation of the yield of cyclohexanol with partition coefficient log P and FMO energy E_{LUMO-b}:

$$\lg k = -1.433 + 0.009 \log P - 0.406 E_{LUMO-b}$$
$$R = 0.968, \quad R^2 = 0.937, \quad F = 44.317, \quad SEE = 0.073 \tag{1}$$

$$\text{Yield}\ (\%) = 9.556 + 0.500 \log P - 8.997 E_{LUMO-b}$$
$$R = 0.812, \quad R_2 = 0.660, \quad F = 5.826, \quad SEE = 4.388 \tag{2}$$

3.4. Validation of the established QSAR models

With a satisfactory QSAR model in hand, chemists should be able to predict the reactivity of the target compound with certainty. In this present investigation, the built models were validated by the experimental data and the calculated data of the cyclohexane hydroxylation catalyzed by ironporphyins. The experimental data (actual lg k and yield (%)) were summarized in Table 4 together with the calculated data (estimated lg k and yield (%)) of Eqs. (1) and (2) and the residual values between them are listed as well.

When $R^2 = 0.937$ and SEE = 0.073, it seems that a perfect model equation was obtained with Eq. (1). Amazingly the residual for the actual data and estimated data of lg k were distributed normally around ±0.1 in Table 4. And the plot of the actual data versus the estimated data (Fig. 2) also told us that the estimated lg k values seem to fit the actual lg k values very well. Thus the relationship of the rate constant and the structure descriptors of ironporphyrins could be quantified reliably by Eq. (1). Compared with Eq. (1), the linear correlation of Eq. (2) is not as good as Eq. (1) and the residual values between the estimated and the actual yield (%) of cyclohexanol were somewhat larger with squared correlation coefficient $R^2 = 0.660$. This larger deviation was mainly caused by the further oxidation of cyclohexanol. The experimentally observed cyclohexanol yield (%) was somewhat lower than the real yield (%) of the

Table 3
Pearson correlation matrix of the parameters.

	lg *k*	Yield (%)	log *P*	E_{HOMO-a}	E_{HOMO-b}	E_{LUMO-a}	E_{LUMO-b}	DELH
lg *k*	1							
Yield (%)	0.811	1						
log *P*	−0.165	0.030	1					
E_{HOMO-a}	0.392	0.505	0.120	1				
E_{HOMO-b}	−0.772	−0.452	0.336	0.245	1			
E_{LUMO-a}	−0.280	−0.157	0.425	0.515	0.705	1		
E_{LUMO-b}	−0.964	−0.792	0.259	−0.468	0.733	0.348	1	
DELH	−0.797	−0.757	0.090	−0.849	0.296	−0.072	0.863	1

Table 4
Actual estimated lg *k*, yield (%) and residual based on Eqs. (1) and (2).

TRPPFe^{III}Cl catalyst	lg *k*			Yield (%)		
	Actual	Estimated	Residual	Actual	Estimated	Residual
1	−0.0046	0.0116	−0.0162	42.85	41.88	0.97
2	−0.6478	−0.6216	−0.0262	20.05	27.37	−7.32
3	−0.5408	−0.6502	0.1094	30.50	27.22	3.28
4	−0.5604	−0.4580	−0.1024	29.14	31.80	−2.66
5	−0.5780	−0.6154	0.0374	26.53	28.88	−2.35
6	−0.7364	−0.7215	−0.0149	24.35	26.09	−1.74
7	−0.8146	−0.7437	−0.0709	27.85	24.22	3.63
8	−0.7496	−0.7112	−0.0384	31.20	27.18	4.02
9	−0.3302	−0.3641	0.0339	35.04	32.84	2.20

cyclohexane hydroxylation reaction. Consequently, Eq. (2) could not describe the quantitative relationship of the cyclohexanol yield and the structure descriptors of ironporphyrin very well. (All of the MLR analysis and correlation analysis mentioned above were performed by the statistics software package SPSS 12.0 version developed by the Apache Software Foundation.)

3.5. Molecular graphics studies and Mulliken's electron population analysis of ironporphyrins

Each molecular descriptor interpreted in QSAR model should have some chemical or physical significance. According to the results of correlation analysis in Table 3, the rate constant lg *k* has a good linear relationship with cyclohexanol yield ($R = 0.811$). It means that cyclohexanol yield would be increased with larger rate constant for the ironporphyrin-catalyzed cyclohexane hydroxylation reaction. Higher lg *k* is also predicted by a large negative HOMO energy E_{HOMO-b} ($R = -0.772$, negative HOMO-b energies are computed). By investigating different substituents at *meso*-phenyl-moiety, it becomes clear that electron withdrawing groups such as halide atoms and nitro-group were predicted to have a beneficial effect on lg *k* value, and similar trend was noticed in Refs. [30,31]. Because the auto-oxidation of metalloporphyrin catalyst is one of the major pathways for catalyst deactivation, ironporphyrin molecules bearing electron withdrawing groups would be more stable since their HOMO energy levels are decreased and the oxygenolysis of ironporphyrin is more difficult. As such ironporphyrin would be more robust towards activating the oxidant. So lower E_{HOMO-b} can lead to larger rate constant and better catalytic activities of ironporphyrins. Besides E_{HOMO-b}, a larger FMO energy a gap value (DEHL) also has negative influence on lg *k* and yield (%) with the negative correlation coefficient listed in Table 3.

From the Pearson correlation matrix in Table 3, E_{LUMO-b} has the strongest correlation with lg *k* and yield (%) ($R = -0.964$). The coefficient absolute values of E_{LUMO-b} in the QSAR model equations (1) and (2) were far greater than the corresponding coefficient absolute values of log *P*, while E_{LUMO-b} and log *P* were in the same order of magnitude. One can conclude that the most important descriptor which affected lg *k* and yield (%) was E_{LUMO-b}. Fig. 3 depicted the plot of linear correlation between lg *k*, yield (%) and E_{LUMO-b} together with squared correlation coefficient. From the graph, it is reasonable to predict that lower E_{LUMO-b} would lead to higher lg *k* and yield (%) which means better catalytic activities for the iron-

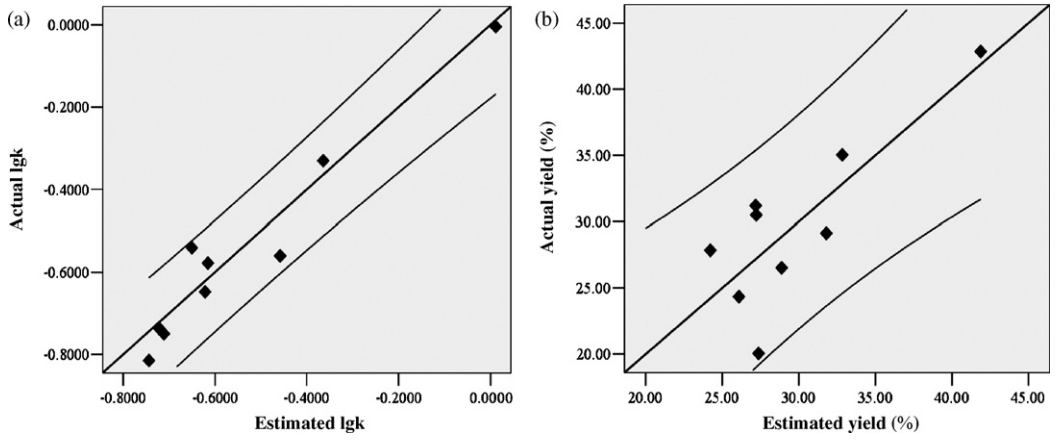

Fig. 2. Plots of actual active data versus estimated active data. Validation of Eq. (1) (a) and validation of Eq. (2) (b) (two side lines express the confidence interval of 95%).

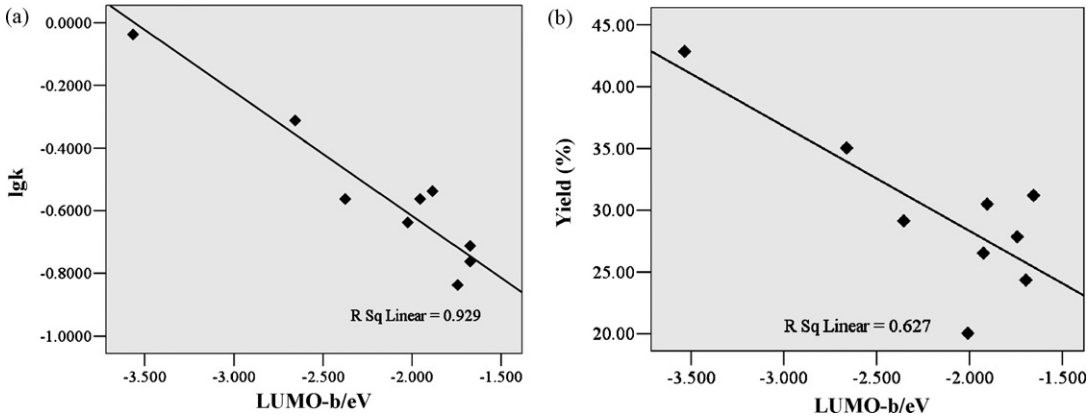

Fig. 3. Plots of $E_{LUMO\text{-}b}$ versus lg k and yield (%). (a) Linear correlation between lg k and $E_{LUMO\text{-}b}$ and (b) linear correlation between yield (%) and $E_{LUMO\text{-}b}$.

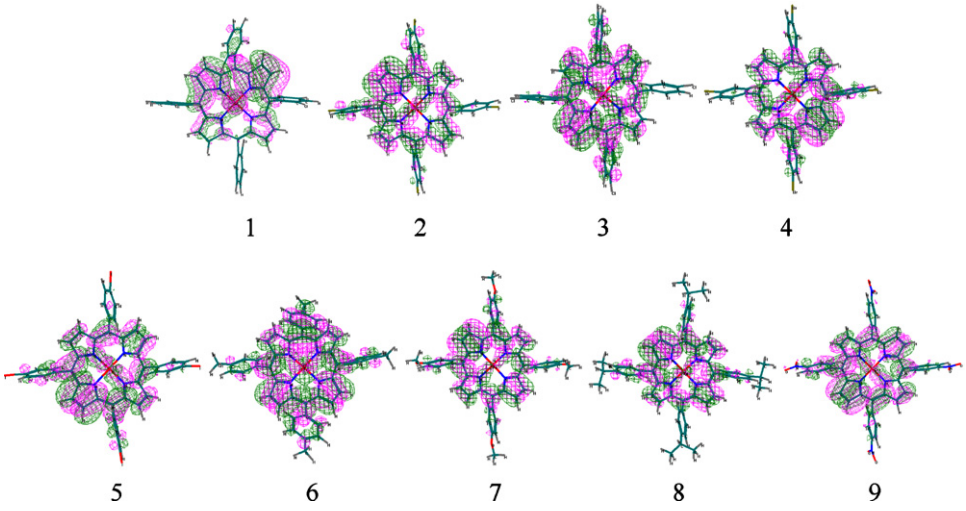

Fig. 4. Density of probability of the LUMO-b for nine irontetraphenylporphyrin derivatives.

porphyrin catalysts. This conclusion had never been found in the published works.

According to the frontier molecular orbital theory, the electron density transfer occurred mainly between the HOMO and LUMO of the reactants in chemical reactions. Smaller energy gap between LUMO and HOMO of the two reactants would make the electron density transfer more easily. In the reaction of cyclohexane oxidation with PhIO catalyzed by substituted ironporphyrins, the oxidant PhIO is activated by ironporphyrin at first. With PhIO close to the molecule surface of ironporphyrin, the LUMO of ironporphyrin molecule works as an electron acceptor to accept the electron density from the HOMO of PhIO. The energy gap was about −7.470 eV based on our quantum chemical calculation result at PM3 level. As the data listed in Table 1, $E_{LUMO\text{-}b}$s of ironporphyins are in the range of −1.655 eV to −3.535 eV. With the lowering of $E_{LUMO\text{-}b}$ of ironporphyin, the energy gap between itself and the E_{HOMO} of PhIO was also decreased. Thus, the electron transfer between the FMO of PhIO and ironporphyin could occur with lower energy barrier. So the activation of PhIO by ironporphyrin was more rapid, which resulted in higher catalytic activities of ironporphyrins.

We have reported that the rate constant lg k, the yield of the cyclohexane hydroxylation have good linear relationships with the substituent constants σ with the substituents on the *para* position and the *meta* position [33]. In this work, we have found that $E_{LUMO\text{-}b}$, which was heavily influenced by substituting groups on *meso*-phenyl ring, was the most important factor affecting the value of lg k and the yield (%). To elucidate the relationship between $E_{LUMO\text{-}b}$, *meso*-substituting group and the catalytic activity of ironporphyrins, a detailed electronic analysis of the metalloporphyrins was performed. Fig. 4 depicted the density of probability of each LUMO-b orbital for nine irontetraphenylporphyrin derivatives. The LUMO orbitals of ironporphyrins were mainly composed of the atomic orbitals of the atoms on the porphin ring, *meso*-phenyl group and the 3d orbitals of the center iron atom. It showed that the substituting groups on *meso*-phenyl do have significant electronic effects on the porphin ring.

Table 5 showed the average values of atomic charges of N atoms (*N*p) and C atoms (C_{meso}, C_α, C_β) on the porphin ring as well as the substituent constants σ (the subsituents on the *para* positon of the *meso*-phenyl ring). The correlation analysis results showed that the positive charges of *N*p have strong linear relationship with

Table 5
The calculated Mulliken's charges of atoms of the ironporphyrin ring.

TRPPFe^{III}Cl	*N*p	C_{meso}	C_α	C_β	σ
1	0.5474	0.0913	−0.1060	−0.2417	–
2	0.4127	0.1536	−0.1102	−0.2393	0.06
3	0.3974	0.1625	−0.1275	−0.2226	0.23
4	0.3904	0.0772	−0.1069	−0.1662	0.23
5	0.3776	0.1623	−0.1011	−0.2594	0.18
6	0.3988	0.1794	−0.1202	−0.2397	−0.17
7	0.3436	0.1824	−0.1131	−0.2567	−0.27
8	0.3439	0.1791	−0.1218	−0.2391	−0.15
9	0.4699	0.1489	−0.1001	−0.2523	0.78

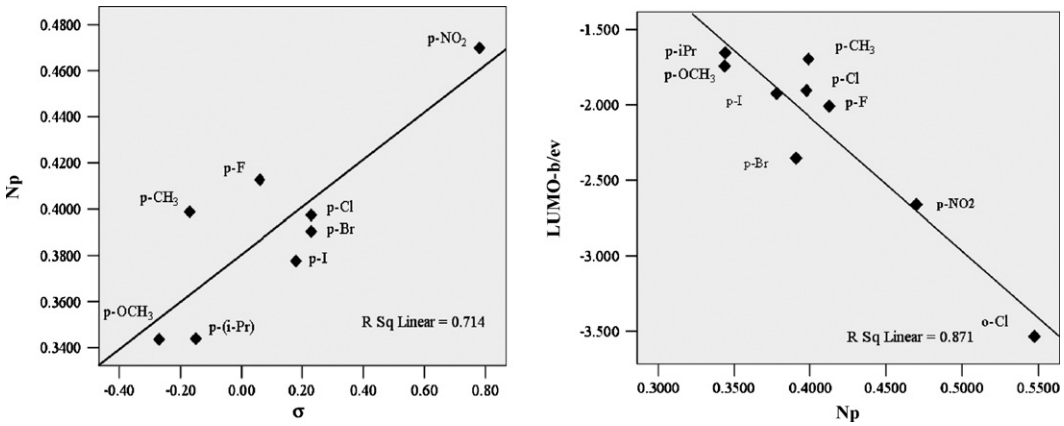

Fig. 5. Plots of *N*p charges versus σand E_{LUMO-b}.

σ and E_{LUMO-b}. The plots of *N*p charges versus σ and E_{LUMO-b} were shown in Fig. 5. It is obvious that the positive charges of *N*p increased when electron withdrawing groups (with large σ value) were introduced on the *meso*-phenyl ring. As we known, the increase of the positive charges of *N*p could disperse the electron density around the centro-metal core of ironporphyrin, which was beneficial to ironporphyrin's binding with the oxidant. At the same time, electron withdrawing groups also lead to the decrease of the energy level of E_{LUMO-b}. The analysis above all may explain why ironporphyrin's binding with the oxidant was facilitated and, consequently increases the catalytic activity of ironporphyrin.

3.6. *Effect of partition coefficient log P on the catalytic activities of ironporphyrins*

Another piece of important information gained from Eqs. (1) and (2) is that the partition coefficient log *P* of ironporphyrin can affect the catalytic activities of ironporphyrin as well. The value of log *P* represented the proportion of solute in the organic solution (n-octane) and water. Typically the values of log *P* of the lipophilic solutes are larger than the hydrophilic solutes. Since Eqs. (1) and (2) show that both lg *k* and yield (%) increase when log *P* is increased, the increase of the lipophilicity of ironporphryin would favorably affect the reaction rate and the cyclohexanol yield. As we have mentioned previously that log *P* and E_{LUMO-b} were in the same order of magnitude, the weight of log *P* was less than E_{LUMO-b} in Eqs. (1) and (2), and manifested that the main element affected ironporphyrin's catalytic activity was still E_{LUMO-b}.

4. Conclusion

In summary, QSAR studies had been applied to investigate the cyclohexane hydroxylation reaction catalyzed by nine iron-tetraphenylporphyrin derivatives. Bi-parametric QSAR model equations for the rate constant and cyclohexanol yield had been built, respectively, by MLR analysis. Several important lesson were gained form the QSAR models: (1) the frontier molecular orbital energy E_{LUMO-b} of ironporphyrin molecules has the most pronounced effect on the catalytic activities; (2) the variation of LUMO was controlled by the electronic effect of substituting groups on the *meso*-phenyl ring. Electron withdrawing groups should be able to disperse the electron density around the centro-metal core of porphyrins, thus decreasing E_{LUMO-b}. With the energy gap between the LUMO of ironporphyrin and the HOMO of PhIO decreased, the activation reaction of PhIO by ironporphyrins was faster. This term will facilitate cyclohexane hydroxylation and the catalytic activity of ironporphyin catalyst was enhanced; (3) the partition coefficient log *P* does affect the reaction to a smaller extent and this indicated that the solubility of the catalyst is important too. Catalyst with better solubility in organic liquid phase could better catalyze the cyclohexane hydroxylation reaction under the tested reaction conditions. We believe that all these information can be useful in the future for the design of better metalloporphyrin catalyst for hydrocarbon oxidations.

Acknowledgement

The authors gratefully thank the financial supports of National Natural Science Foundation of China (Grants CN J0830415, 20502005).

References

[1] B. Meunier, Chem. Rev. 92 (1992) 1411.
[2] J.T. Groves, T.E. Nemo, R.S. Myers, J. Am. Chem. Soc. 101 (1979) 1032.
[3] J.T. Groves, T.E. Nemo, J. Am. Chem. Soc. 105 (1983) 6243.
[4] J.T. Groves, R.J. Quinn, J. Am. Chem. Soc. 107 (1985) 5790.
[5] T.G. Traylor, K.W. Hill, W.P. Hann, S. Tsuchiya, B.E. Dunlap, J. Am. Chem. Soc. 114 (1992) 1308.
[6] W.W. Nam, H.J. Lee, S.Y. Oh, C. Kim, H.G. Jang, J. Inorg. Biochem. 80 (2000) 219.
[7] T. Takai, E. Hata, K. Yorozu, Chem. Lett. (1992) 2077.
[8] E.R. Birnbaum, M.W. Grinstaff, J.A. Labinger, J.E. Bercaw, H.B. Gray, J. Mol. Catal. A: Chem. 104 (1995) 119.
[9] E.R. Birnbaum, J.A. Labinger, J.E. Bercaw, H.B. Gray, Inorg. Chim. Acta 270 (1998) 433.
[10] C.C. Guo, H.P. Li, J.B. Xu, J. Catal. 185 (1999) 345.
[11] C.C. Guo, G. Huang, X.B. Zhang, D.C. Guo, Appl. Catal. A: Gen. 247 (2003) 261.
[12] R.R.L. Martins, M.G.P.M.S. Neves, A.J.D. Silvestre, M.M.Q. Simoes, J. Mol. Catal. A: Chem. 172 (2001) 33.
[13] R.R.L. Martins, M.G.P.M.S. Neves, A.J.D. Silvestre, M.M.Q. Simoes, J. Mol. Catal. A: Chem. 137 (1999) 41.
[14] J. Lee, J.A. Hunt, J.T. Groves, J. Am. Chem. Soc. 120 (1998) 7493.
[15] M.S. Liao, J.D. Watts, M.J. Huang, J. Phys. Chem. A 109 (2005) 11996.
[16] K.M. Kadish, F. D'Souza, A. Villard, M. Autret, E.V. Caemelbeck, P. Bianco, A. Antonini, P. Tagliatesta, Inorg. Chem. 33 (1994) 5169.
[17] H.L. Chen, P.E. Ellis, T. Wijesekera, T.E. Hagan, S.E. Groh, J.E. Lyons, D.P. Ridge, J. Am. Chem. Soc. 116 (1994) 1086.
[18] S.W. Lai, Y.J. Hou, C.M. Che, H.L. Pang, K.Y. Wong, C.K. Chang, N. Zhu, Inorg. Chem. 43 (2004) 3724.
[19] W.R. Scheidt, C.A. Reed, Chem. Rev. 81 (1981) 543 (and references therein).
[20] F.S. Vinhado, P.R. Martins, A.P. Masson, D.G. Abreu, E.A. Vidoto, O.R. Nascimento, Y. Iamamoto, J. Mol. Catal. 188 (1–2) (2002) 141.
[21] T. Saitoh, T. Ikeue, Y. Ohgo, M. Nakamura, Tetrahedron 53 (1997) 12496.
[22] S.A. Hassan, H.A. Hassan, K.M. Hashem, H.M. Abdel Dayem, Appl. Catal. A: Gen. 300 (2006) 14.
[23] P.E. Ellis Jr., J.E. Lyons, Coord. Chem. Rev. 105 (1990) 181.
[24] J.E. Lyons, P.E. Ellis Jr., H.K. Myers Jr., J. Catal. 155 (1995) 59.
[25] J. Haber, L. Matachowski, K. Pamin, J. Poltowicz, J. Mol. Catal. A: Chem. 198 (2003) 215.
[26] M. Karelson, V.S. Lobanov, Chem. Rev. 96 (1996) 1027.
[27] S.P. Gupta, P. Singh, M.C. Bindal, Chem. Rev. 83 (1983) 633.
[28] C. Hansch, A. Leo, D. Hoekman, J. Am. Chem. Soc. 117 (1995) 9782.
[29] C. Hansch, A. Kurup, R. Garg, H. Gao, Chem. Rev. 101 (2001) 619.
[30] Q.Z. Lü, R.Q. Yu, G.L. Shen, J. Mol. Catal. A: Chem. 198 (2003) 9.

[31] Y.H. Zhang, Y.B. She, R.G. Zhong, X.T. Zhou, H.B. Ji, Acta Chim. Sin. 62 (2004) 2228.
[32] C.C. Guo, G. Huang, D.C. Guo, Kinet. Catal. 47 (2006) 93.
[33] C.C. Guo, J. Catal. 178 (1998) 182.
[34] C.C. Guo, M.F. Chu, Q. Liu, Y. Liu, D.C. Guo, X.Q. Liu, Appl. Catal. A: Gen. 246 (2003) 303.
[35] C.C. Guo, Q. Liu, X.B. Zhang, CN 1269343.A (2000).
[36] H.J. Lucas, E.R. Kennedy, J.R. Johnson, M.W. Formo, Organic Synthesis, Coll., vol. 3, John Wiley and Sons, Inc., New York, 1995, p. 482.
[37] A.D. Adler, F.R. Longo, F. Kampas, J. Kim, J. Inorg. Nucl. Chem. 32 (1970) 2443.
[38] K. Anzai, K. Hatano, Y.J. Lee, W.R. Scheidt, Inorg. Chem. 20 (1981) 2337.
[39] C. Maricondi, W. Swift, D.K. Straub, J. Am. Chem. Soc. 91 (1969) 5205.
[40] A.D. Adler, F.R. Longo, J.D. Finarelli, J. Org. Chem. 32 (1976) 476.
[41] J.S. Lindscy, I.C. Schreiman, H.C. Hsu, J. Org. Chem. 52 (1987) 827.
[42] D.X. Jian, C. Gu, M.D. Gui, Chem. J. Chin. Univ. 16 (1995) 909.
[43] H. Kobayashi, T. Higuchi, Y. Kaizu, H. Osada, M. Aoki, Bull. Chem. Soc. Jpn. 48 (1975) 3137.
[44] L.Z. Wang, Y.B. She, R.G. Zhong, Org. Process Res. Develop. 10 (2006) 757.
[45] L.Y. Liu, C.C. Guo, Chin. J. Anal. Chem. 21 (1993) 472.
[46] C.C. Guo, M.D. Gui, S.J. Zhu, Chin. J. Org. Chem. 14 (1994) 163.
[47] C.C. Guo, S.J. Zhu, M.D. Gui, Acta Chim. Sin. 50 (1992) 129.
[48] M.D. Petersen, S.V. Boye, E.H. Nielsen, S. Sinning, O. Wiborg, M. Bols, Bioorg. Med. Chem. 15 (2007) 4159.
[49] C. Hansch, Structure–Activity Relationship [M], Dergomon Elmsford, New York, 1973.
[50] K. De, C. Sengupta, K. Roy, Bioorg. Med. Chem. 12 (2004) 3323.
[51] Q.L. Wei, S.S. Zhang, J. Gao, Bioorg. Med. Chem. 14 (2006) 7146.